Commun Nonlinear Sci Numer Simulat 15 (2010) 1358–1367

Contents lists available at ScienceDirect

Commun Nonlinear Sci Numer Simulat

journal homepage: www.elsevier.com/locate/cnsns

Hard versus soft impacts in oscillatory systems modeling

Barbara Blazejczyk-Okolewska *, Krzysztof Czolczynski, Tomasz Kapitaniak

Division of Dynamics, Technical University of Lodz, Stefanowskiego 1/15, 90-924 Lodz, Poland

ARTICLE INFO

Article history:
Received 26 February 2009
Received in revised form 12 May 2009
Accepted 12 May 2009
Available online 27 May 2009

PACS:
46.40.−f
05.45.−a

Keywords:
Modeling of collisions
Hard impacts
Soft impacts
Cantilever beam
Periodic motion
Co-existing attractors

ABSTRACT

The applicability of the soft and hard impact models in modeling of vibro-impact systems is discussed in the paper. We derive the conditions which allow the same rate of energy dissipation in dynamical systems which use both impact models. The advantages and disadvantages of both models in modeling are discussed. We show that in the case of the stiff base both methods give the same results but the elastic base application of the hard impact model leads to wrong results.

1. Introduction

Recently, one observes the growing interest in the dynamics of impacting systems as there is a large number of mechanical systems of practical interest in which the impacting motion occurs between elements. The fundamental nature of the impacting motion, and the resulting dynamical phenomena become a matter of great interest. Extensive studies of vibro-impact systems started in the second half of the XXth century with the works of Kobrynskii [1], Feigin [2], Fillippov [3] and Peterka [4]. During recent years considerable interest in such systems has been seen, particularly applied to one degree-of-freedom piece-wise linear systems excited by external periodic force. The investigations by Shaw and Holmes [5], Nordmark [6], Blazejczyk et al. [7], Lenci and Rega [8], Hogan [9], Budd and Dux [10], Chin et al. [11] and DiBernardo et al. [12] can serve as examples.

One of the problem of the modeling of the vibro-impact systems is the selection of the appropriate impact model. In the simplest way one assumes infinitely small time of the bodies contact at the collision and constant value of the restitution coefficient describing the energy dissipation. This model is based on the Newton's law of impact and is called *hard impact model*. In this model the rigid body collides with stiff base and both the colliding body and the base are not deformed at the collision. The consideration of the finite nonzero contact time and a penetration of the base by the colliding body leads to the *soft impact model*. In this model the impacting base (fender) is cushioned with a spring-damper support as it is common in engineering. A soft impact model allows the application of different types of spring dampers support, which can be either linear or nonlinear. The application of soft impact models to various engineering application is discussed in the works [13–16].

* Corresponding author. Tel.: +4842 6312231; fax: +4842 6365646.
E-mail address: okolbar@p.lodz.pl (B. Blazejczyk-Okolewska).

1007-5704/$ - see front matter © 2009 Elsevier B.V. All rights reserved.
doi:10.1016/j.cnsns.2009.05.046

In this paper we discuss the applicability of soft and hard impact models in modeling of the vibro-impact systems. We derive the conditions under which both methods are equivalent in the sense of the same rate of energy dissipation. The advantages and disadvantages of both models are discussed. We show that in the case of the stiff base both methods give the same results but for the elastic base the application of a hard impact model leads to wrong results.

This paper is organized as follows. In Section 2 we describe hard and soft impact models and derive the condition which allows the same rate of energy dissipation in both models. Section 3 presents the main differences in the dynamical behavior of the ball (material point) which collides with the parallel base when hard and soft impacts are considered. The influence of the impact modeling on the dynamics of two degree-of-freedom system is discussed in Section 4. Finally, we summarize our results in Section 5.

2. Impact models

Collision of the rigid body with mass m_1 with the base can be modeled in two ways. The first one (hard impacts) assume that: (i) both the colliding body and the base are stiff, (ii) the time of the collision (the time of the contact of two bodies) τ_i is equal to zero, (iii) there exists the following relation between the velocity of mass m_1 before the collision (v^-) and its velocity after collision (v^+)

$$v^+ = -k_r v^-, \tag{1}$$

where k_r is a restitution coefficient. Relation (1) is known as Newton's law of impacts. At the hard impact the kinetic energy is dissipated as follows:

$$\frac{E_k}{E_0} = \left(\frac{v^+}{v^-}\right)^2 = k_r^2, \tag{2}$$

where E_0 and E_k denote, respectively, kinetic energy before and after the collision.

The second way of modeling assumes that mass m_1 collides with the base modeled as a light fender supported by a light spring with the restitution coefficient k_s and light viscous damper with the damping coefficient t_s as shown in Fig. 1. Differently to the previous case of hard impacts in this case the time of the collision τ_i is lager than zero and the colliding body can penetrate the base as deeply as h_i. These two differences can result in different dynamical behavior of the vibro-impact systems in which hard and soft impacts have been considered.

As we are considering two different models of impacts it is worth to estimate the relation between coefficients k_s, t_s and restitution coefficient k_r which allows the same energy dissipation. Assume that mass m_1 is thrown from height H_0. Its velocity at the moment of the collision is $v_0^- = \sqrt{2gH_0}$, where g is the acceleration due to the gravity. The velocity after the collision is given by Eq. (1) and as the energy is dissipated according to Eq. (2) the maximum height the mass m_1 can reach after the first collision is equal to $H_1 = (k_r)^2 H_0$ and after the successive collisions respectively $H_2 = (k_r)^2 H_1$, $H_3 = (k_r)^2 H_2$,....

To estimate the coefficients k_s and $t_s$in the same way, one has to consider that at the collision of mass m_1 with the base a new oscillatory system shown in Fig. 1 is created. Assuming that coefficient k_s is large enough it is possible to neglect static displacement of the spring $x_g = m_1 g/k_s$, so $x_{st} = 0.0$ is the static equilibrium of this oscillator. Its dynamics is governed by the following equation:

$$m_1 \ddot{x}_s + t_s \dot{x}_s + k_s x_s = 0, \tag{3}$$

and in the dimensionless form

$$\ddot{x}_s + 2h_s \dot{x}_s + \alpha_s^2 x_s = 0 \tag{4}$$

where

$$h_s = \frac{t_s}{2m_1}, \quad \alpha_s^2 = \frac{k_s}{m_1}. \tag{5}$$

The solution of Eq. (4) is as follows:

$$\begin{aligned} x_s &= e^{-h_s \tau}(A \sin \lambda_s \tau + B \cos \lambda_s \tau) \\ \dot{x}_s &= -h_s e^{-h_s \tau}(A \sin \lambda_s \tau + B \cos \lambda_s \tau) + \lambda_s e^{-h_s \tau}(A \cos \lambda_s \tau - B \sin \lambda_s \tau), \end{aligned} \tag{6}$$

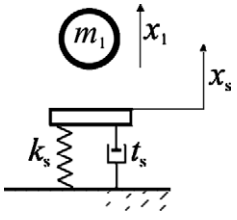

Fig. 1. Soft impact model as massless fender supported by damper and spring.

where

$$\lambda_s = \sqrt{\alpha_s^2 - h_s^2} \tag{7}$$

is the frequency of the damped oscillations. Assuming that the velocity of the colliding body at the collision is given by v_0, one gets the following initial conditions

$$\tau = 0 \Rightarrow x_s = 0, \dot{x}_s = v_0, \tag{8}$$

so Eq. (6) take the form

$$\begin{aligned} x_s &= e^{-h_s\tau}\frac{v_0}{\lambda_s}\sin\lambda_s\tau \\ v_s &= \dot{x}_s = -h_s e^{-h_s\tau}\frac{v_0}{\lambda_s}\sin\lambda_s\tau + \lambda_s e^{-h_s\tau}\frac{v_0}{\lambda_s}\cos\lambda_s\tau. \end{aligned} \tag{9}$$

At the beginning of mass m_1 – fender contact and at its end after time τ_i oscillator (3) is in the equilibrium state so the contact takes place during the time equal to the half of the oscillation period

$$\tau_i = \frac{1}{2}T_i = \frac{\pi}{\lambda_s}. \tag{10}$$

Multiplying both sides of Eq. (3) by velocity v_s one gets

$$m_1 v_s \dot{v}_s = -k_s x_x v_s - t_s v_s^2. \tag{11}$$

The expression

$$m_1 v_s \dot{v}_s = \frac{\mathrm{d}}{\mathrm{d}t}\left(\frac{m_1 v_s^2}{2}\right) = \frac{\mathrm{d}E_k}{\mathrm{d}t} \tag{12}$$

represents the time derivative of the kinetic energy of mass m_1. At the contact of duration $0.5T_i$ the energy dissipation is given by

$$\Delta E_k = \int_0^{0.5T_z} \mathrm{d}E_k = \int_0^{0.5T_i} -k_s x_s v_s \mathrm{d}\tau + \int_0^{0.5T_i} -t_s v_s^2 \mathrm{d}\tau = \Delta E_{k1} + \Delta E_{k2}. \tag{13}$$

The first integral ΔE_{k1} which represents energy dissipation in the spring is equal to zero as at the beginning and at the end of the contact the length of the spring is the same. This observation leads to the conclusion that in the lack of damping ($t_s = 0$), for any value of the stiffness coefficient k_s soft collision is equivalent to the ideal elastic hard collision with restitution coefficient $k_r = 1.0$. Different values of k_s give different collision times and different base penetration depth which allows the modeling of the collisions between rigid and elastic bodies, for example collision of the stiff steel ball with elastic block of elastomer.

Substituting Eq. (9) into the second integral of Eq. (13) one gets

$$\Delta E_{k2} = \int_0^{\pi/\lambda_s} -t_s\left(-h_s e^{-h_s\tau}\frac{v_0}{\lambda_s}\sin\lambda_s\tau + \lambda_s e^{-h_s\tau}\frac{v_0}{\lambda_s}\cos\lambda_s\tau\right)^2 \mathrm{d}\tau = -t_s\frac{v_0^2}{\lambda_s^2}\frac{h_s^2+\lambda_s^2}{4h_s}(1 - e^{-2\pi/\lambda_s}), \tag{14}$$

and

$$\Delta E_{k2} = -\frac{m_1 v_0^2}{2}(1+\zeta^2)(1 - e^{-2\pi\zeta}) \tag{15}$$

where

$$\zeta = \left(\frac{h_s}{\lambda_s}\right)^2 = \frac{h_s^2}{\alpha_s^2 - h_s^2}. \tag{16}$$

Eq. (15) show that the amount of the energy dissipated at the soft collision depends on the value of the parameter ζ. Assuming that h_s is much smaller than α_s, Eq. (16) can be approximately rewritten as

$$\zeta = \frac{h_s^2}{\alpha_s^2 - h_s^2} \approx \frac{h_s^2}{\alpha_s^2} = \frac{t_s^2 m_1}{4m_1^2 k_s} = \frac{1}{4m_1^2}\frac{t_s^2}{k_s}. \tag{17}$$

Eq. (17) shows that the amount of energy dissipated for two different bases is the same (which is equivalent with the preservation of the same restitution coefficient in the hard impact model) when the following relation is fulfilled

$$\left(\frac{t_{s2}}{t_{s1}}\right)^2 = \frac{k_{s2}}{k_{s1}}, \tag{18}$$

where subscripts 1 and 2 denote, respectively, base 1 and 2 so for example increasing the stiffness four times one has to increase the damping twice.

Denoting kinetic energy of the colliding body before and after the impact respectively as E_k^- and E_k^+, one gets

$$E_k^+ = E_k^- + \Delta E_{k2} = E_k^-(1 - (1+\zeta^2)(1 - e^{-2\pi\zeta})), \tag{19}$$

and equivalent restitution coefficient:

$$k_r = \sqrt{\frac{E_k^+}{E_k^-}} = \sqrt{(1 - (1+\zeta^2)(1 - e^{-2\pi\zeta}))}. \tag{20}$$

The relation between parameters k_r and ζ^2 given by Eq. (20) is described in Fig. 2(a). The increase of the damping coefficient t_s results in the decrease of the equivalent restitution coefficient k_r.

Eqs. (16) and (20) allow the determination of the base parameters α_s and h_s equivalent to the given value of the restitution coefficient k_r. Fig. 2(b) shows the values of h_s versus α_s^2 for $k_r = 0.1, 0.2, \ldots, 0.9$. The example of the relation between k_r and h_s for given values of α_s^2 and the dependence of the contact time τ_i on the parameters h_s and α_s given by

$$\tau_i = \frac{1}{2}T_i = \frac{\pi}{\lambda_s} = \frac{\pi}{\sqrt{\alpha_s^2 - h_s^2}}, \tag{21}$$

is shown in Fig. 2(c). It should be mentioned here that Eq. (21) is valid under the previously made assumption that coefficient k_s is large enough to neglect static displacement of the spring, i.e., $x_{st} = 0.0$ is the static equilibrium of this oscillator. For very soft base one has to consider that the contact time τ_i is larger than the value given by Eq. (21). Table 1 presents the values of parameters h_s and α_s^2 equivalent to the restitution coefficients $k_r = 0.6$ and $k_r = 0.9$.

3. Comparison of soft and hard impact models

To compare two impact models consider the collision of the mass $m_1 = 1.0$ thrown from the height $H_0 = 1.0$ which collides with the horizontal base. The results of our calculations are shown in Fig. 3(a–c) (restitution coefficient $k_r = 0.9$) and Fig. 4(a and b) (restitution coefficient $k_r = 0.6$). Fig. 3(a) shows the time series of the mass displacement $x_1(\tau)$. The grey line represents the results obtained using hard impact model (restitution coefficient $k_r = 0.9$). Notice that the successive maximum heights H_i, fulfill condition $H_i = k_r^2 H_{i-1}$. The black line denotes the same time series calculated for the soft impact model with the following parameters: $\alpha_s^2 = 20,000,\ h_s = 4.74$ (see Table 1). For $m_1 = 1.0$, the stiffness and damping parameters of the

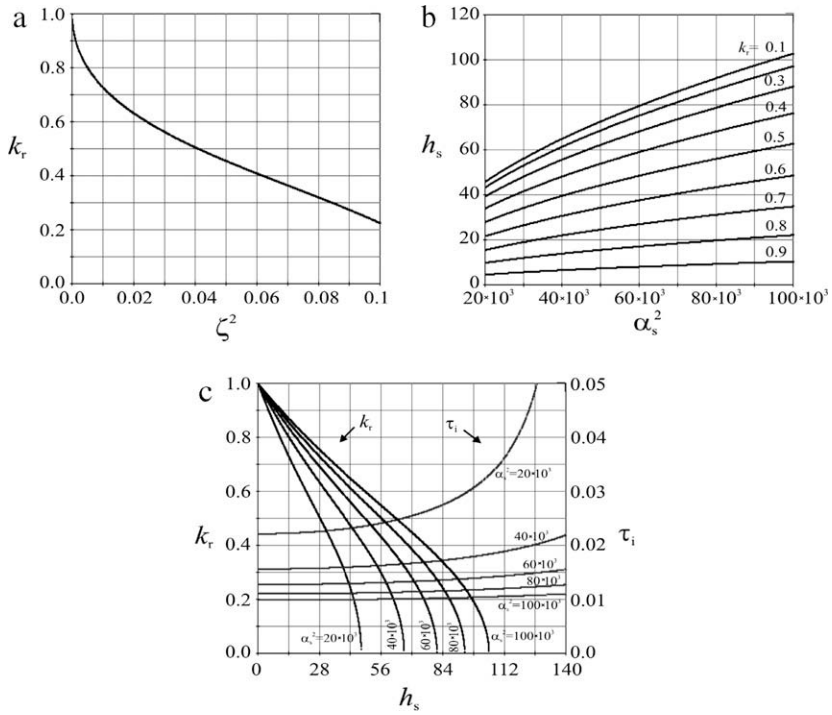

Fig. 2. Relations between parameters $k_r, \alpha_s^2, h_s, \zeta$ and τ_i in hard and soft impact models.

Table 1
Values of the damping coefficient h_s and base eigenfrequency α_s^2 equivalent, respectively, to the restitution coefficients $k_r = 0.6$ and $k_r = 0.9$.

k_r	α_s^2	h_s
0.6	100,000	48.75
	20,000	21.81
	2000	6.9
	100	1.55
	10	0.488
0.9	100,000	10.59
	20,000	4.74
	2000	1.5
	100	0.34
	10	0.106

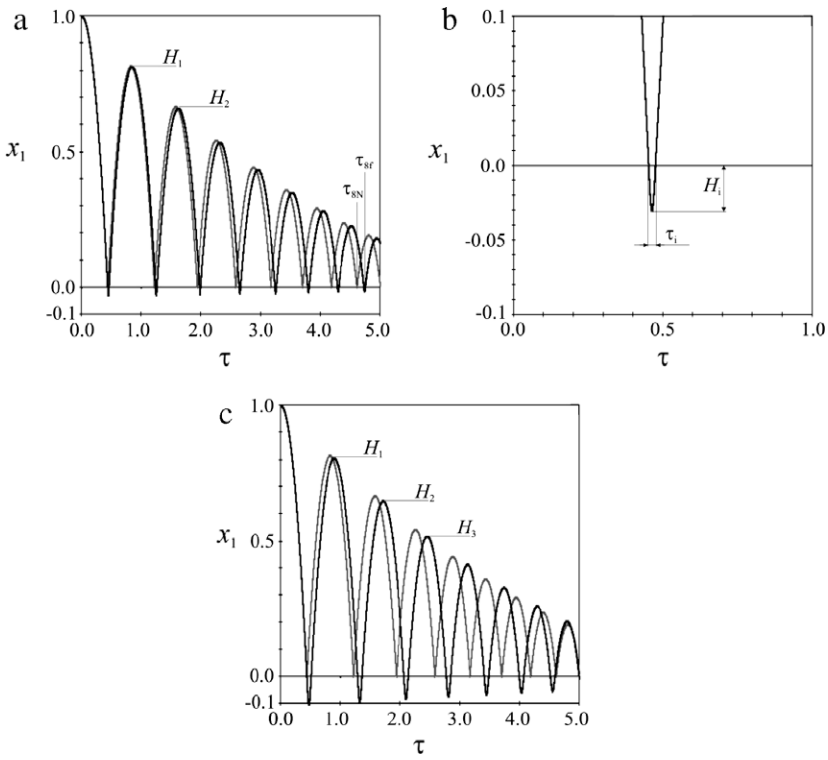

Fig. 3. Time series of the mass m_1 displacement $x_1(\tau)$; soft impacts (black line), hard impacts (grey line): (a) $k_r = 0.9,\ \alpha_s^2 = 20,000,\ h_s = 4.75$, (b) details of the first collision, (c); $k_r = 0.9,\ \alpha_s^2 = 2000,\ h_s = 1.5$.

oscillator created by the colliding body and the fender are, respectively, $k_s = 20{,}000$ and $t_s = 9.48$. As according to our assumptions in both cases the energy dissipation is the same, and a static displacement of the spring with high stiffness k_s is small, the maximum heights H_i of the impacting body are approximately the same in both cases. Nonzero contact time in the soft impact model implies that the successive collisions do not occur in the same time, the eighth collision (the last one shown in Fig. 3(a)) occurs after the time $\tau_{8f} = 4.73$, which is larger than the equivalent time $\tau_{8N} = 4.6$ in hard impact case by 2.6% The first collision in the soft impact model is show in Fig. 3(b). Its duration time is $\tau_i = 0.0225$, and a penetration depth is $H_i = 0.0302$. The results for more stiff base described by parameters $\alpha_s^2 = 2000,\ h_s = 1.5$ are show in Fig. 3(c). Notice that in this case the duration of the first collision increases to $\tau_i = 0.073$, and the penetration depth to $H_i = 0.099$. The duration of the eighth collision (no more visible in the scale of the figure) is $\tau_{8f} = 5.06$. During the collision with the base of the low stiffness, the static displacement of the fender $H_{s0} = m_1 g/k_s \approx 0.005$ cannot be neglected. As the result of this maximum height H_i of the colliding body after successive impacts are smaller than in the model with hard impacts and equal to $H_1 = 0.8$ (0.81), $H_2 = 0.63$ (0.656), $H_3 = 0.5$ (0.53), etc. The results in brackets are for the model with hard impacts.

Fig. 4(a and b) shows the time series of the mass displacement $x_1(\tau)$. The grey line represents the results obtained using the hard impact model (restitution coefficient $k_r = 0.6$). Notice that the successive maximum heights H_i, fulfill condition $H_i = k_r^2 H_{i-1}$. The black line in Fig. 4(a) denotes the same time series calculated for the soft impact model with the following

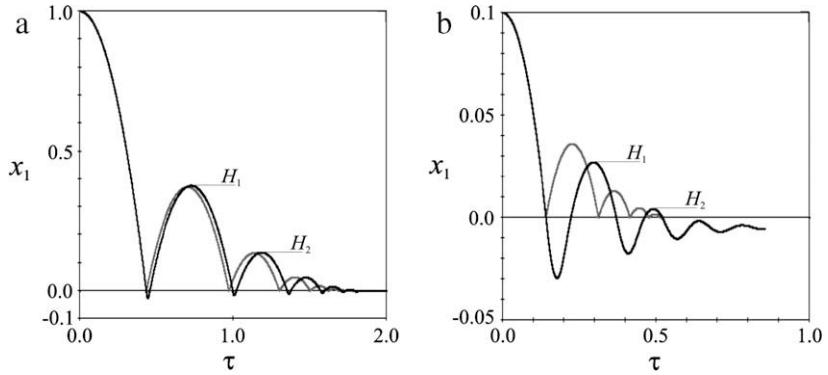

Fig. 4. Time series of mass m_1 displacement x_1 (τ); soft impacts (black line), hard impacts (grey line): (a) $k_r = 0.6,\ \alpha_s^2 = 20,000, h_s = 21.81$, (b) $k_r = 0.6,\ \alpha_s^2 = 2000,\ h_s = 6.9$.

parameters: $\alpha_s^2 = 20,000$ and $h_s = 21.81$. As in the previous case (Fig. 3(a)) the successive maximum heights H_i ($H_1 = 0.36$, $H_2 = 0.13\ldots$) fulfill condition $H_i = k_r^2 H_{i-1}$. Nonzero duration time of the successive collisions in the soft impact model results in the collision delay. The results obtained for $\alpha_s^2 = 2000,\ h_s = 6.9$ and initial height $H_0 = 0.1$ (which is only 20 times larger than the static displacement of the fender $H_{s0} \approx 0.005$) are presented in Fig. 4(b). As the result of such a small difference between H_0 and H_{s0}, the successive maximum heights H_i ($H_1 = 0.027$ (0.036), $H_2 = 0.004$ (0.013)... where the results in brackets are for the model with hard impacts) are significantly smaller than in the hard impact model.

Our results show that both modeling methods give similar results only in the case when the contact time and penetration depth are sufficiently small, i.e., when the stiffness of the base is sufficiently large. For the bases with lower stiffness one observed a significant difference between the results obtained using soft and hard impact modeling. These differences are created by the external forces acting on the colliding body during the nonzero contact time.

4. Example

As an example consider the oscillations of the two degree-of-freedom system shown in Fig. 5(a). It consists of the light elastic beam of the length l, elasticity modulus E and inertial moment I. Two concentrated masses m_1 and m_2 are connected to the beam. Mass m_1 is placed at the free end of the beam and mass m_2 is located at the distance l_2 from the mounted end. The transversal oscillations of the beam are forced by the harmonic excitation of the frequency η and the amplitude $e\eta^2$, which acts on mass m_1. The viscous damping with the damping coefficients proportional to the masses, respectively, υm_1 and υm_2 is assumed. During the oscillations mass m_1 can collide with the base located at the distance d from the static equilibrium position of the system.

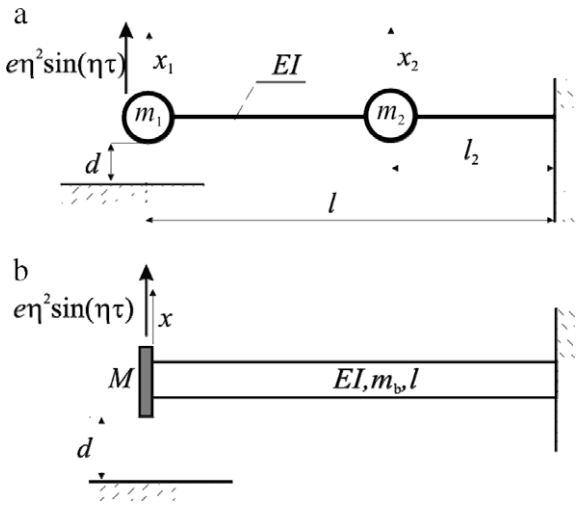

Fig. 5. Cantilever beam with a concentrated mass at its free end: (a) 2DOF model, (b) continuous model with infinite number of DOF.

Table 2
Parameter sets of the considered two degree-of-freedom systems 2DOF-1 and 2DOF-2 shown in Fig. 6(a).

Name	m_1	m_2	l_2	υ	α_1	α_2	M	m_b
2DOF-1	0.92	0.08	0.34	0.23	1.04	28.4	0.9	0.1
2DOF-2	0.28	0.72	0.31	0.23	1.78	11.7	0.1	0.9

In the time intervals between the impacts the equations of motion are as follows:

$$\begin{bmatrix} m_1 & 0 \\ 0 & m_2 \end{bmatrix} \begin{Bmatrix} \ddot{x}_1 \\ \ddot{x}_2 \end{Bmatrix} + \begin{bmatrix} \vartheta m_1 & 0 \\ 0 & \vartheta m_2 \end{bmatrix} \begin{Bmatrix} \dot{x}_1 \\ \dot{x}_2 \end{Bmatrix} + \begin{bmatrix} KB_{11} & KB_{12} \\ KB_{21} & KB_{22} \end{bmatrix} \begin{Bmatrix} x_1 \\ x_2 \end{Bmatrix} = \begin{Bmatrix} e\eta^2 \\ 0 \end{Bmatrix} \sin(\eta t), \tag{22}$$

with the following stiffness matrix

$$\begin{bmatrix} KB_{11} & KB_{12} \\ KB_{21} & KB_{22} \end{bmatrix} = \frac{1}{W} \begin{bmatrix} 12EIl_2^3 & -6EIl_2^2(3l - l_2) \\ -6EIl_2^2(3l - l_2) & 12EIl^3 \end{bmatrix}, \tag{23}$$

where

$$W = 4l^3 l_2^3 - l_2^4(3l - l_2)^2. \tag{24}$$

In the soft impact case as the fender is light, during the collision it is in contact with the colliding mass m_1. Considering this model in the description of the oscillations of the system shown in Fig. 5(a) one has to add coefficients k_s and t_s, respectively, to the stiffness and damping matrixes in Eq. (22) so during the collision the equations of motion are as follow:

$$\begin{bmatrix} m_1 & 0 \\ 0 & m_2 \end{bmatrix} \begin{Bmatrix} \ddot{x}_1 \\ \ddot{x}_2 \end{Bmatrix} + \begin{bmatrix} \vartheta m_1 + t_s & 0 \\ 0 & \vartheta m_2 \end{bmatrix} \begin{Bmatrix} \dot{x}_1 \\ \dot{x}_2 \end{Bmatrix} + \begin{bmatrix} KB_{11} + k_s & KB_{12} \\ KB_{21} & KB_{22} \end{bmatrix} \begin{Bmatrix} x_1 \\ x_2 \end{Bmatrix} = \begin{Bmatrix} e\eta^2 \\ 0 \end{Bmatrix} \sin(\eta t). \tag{23}$$

Our previous studies [17] showed that the considered system of two degree-of-freedom can be considered as an approximation of the class of the infinite dimensional systems, namely the systems with heavy spring elements. Particularly this approximation is very useful in the qualitative identification of the system behavior and estimation of the chaos thresholds.

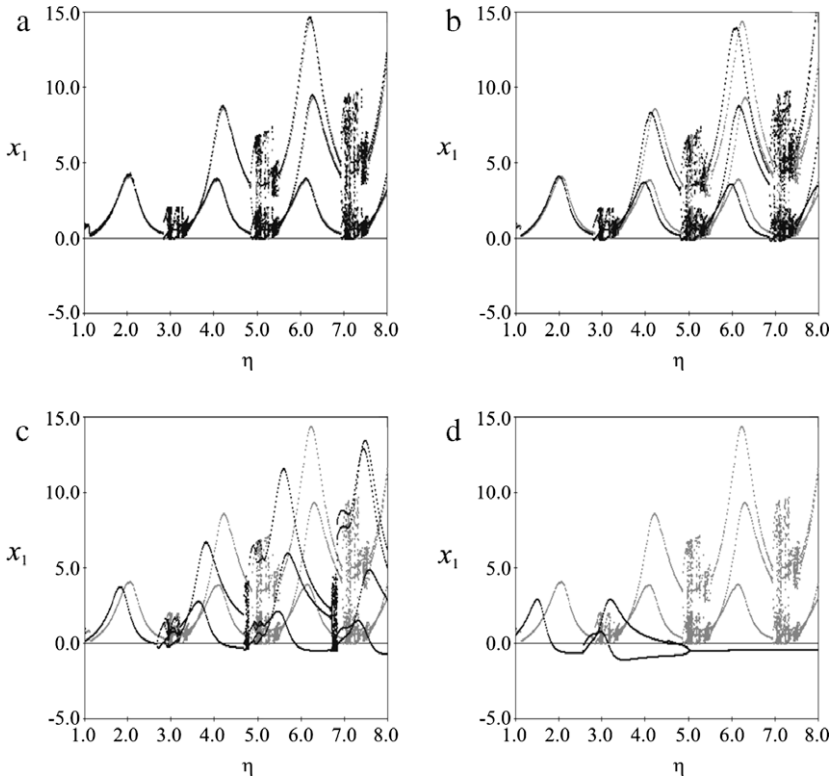

Fig. 6. Bifurcation diagrams showing the displacements of mass x_i observed at the time $t = nT_\eta = 2\pi/\eta$, ($n = 1,2,\ldots$) for 2DOF-1 system ($m_1 = 0.92$ and $m_2 = 0.08$), results for soft impact model with $k_r = 0.6$ are shown in grey, results for soft impact model are shown in black: (a) $\alpha_s^2 = 100,000,\ h_s = 48.75$, (b) $\alpha_s^2 = 2000,\ h_s = 6.9$, (c) $\alpha_s^2 = 100,\ h_s = 1.55$, (d) $\alpha_s^2 = 10,\ h_s = 0.48$.

The system shown in Fig. 5(b) which consists of a heavy beam of mass m_b and mass M placed at its free end. The parameters of the two degree-of freedom system (2DOF) which is equivalent to the infinite dimensional system show in Fig. 5(b) are chosen in the following way:

- stiffness of the beam given by the parameter EI and its length are the same in both cases,
- total masses of both systems are the same, i.e., $m_1 + m_2 = M + m_b$,
- the first two eigenfrequencies α_1 and α_2 are the same for both systems (this can be achieved by the appropriate location of mass m_2, i.e., the selection of the parameter l_2 and appropriate selection of mass ratio m_2/m_1.

More details on this procedure can be found in [17].

In the numerical calculations we consider two sets of parameters denoted respectively as 2DOF-1 and 2DOF-2 which are shown in Table 2. In both cases we consider the same parameters which define the stiffness properties of the beam, i.e., $E = 0.3333$, $I = 1.0$, $l = 1.0$, so the one degree-of-freedom (1DOF) system ($m_1 = 1.0$ and $m_2 = 0.0$) has eigenfrequency α which is equal to 1 ($\alpha^2 = 3EI/m_1 l$). Damping coefficient $\upsilon = 0.23$ has been selected in such a way that the free oscillations decay in the way given by the logarithmic decrement of damping $\Delta = \ln(2)$.

In our numerical calculations we consider system parameters shown in Table 2. We calculated bifurcation diagrams showing the displacements of the mass x_i observed at the time $t = nT_\eta = 2\pi/\eta$, where $n = 1,2,\ldots$ The frequency of external excitation η has been taken as a bifurcation parameter. Fig. 6(a–d) presents the bifurcation diagram for the 2DOF-1 system with $m_1 = 0.92$ and $m_2 = 0.08$. The grey points denote the case of hard impact modeling for $k_r = 0.6$ and $d = 0.0$. Increasing the frequency η one observes qualitatively different dynamical behavior of the system. We observe periodic motion with a period: T_η in the interval $1.11 < \eta < 2.82$, $2T_\eta$ in the interval $3.43 < \eta < 4.86$, $3T_\eta$ in the interval $5.52 < \eta < 6.95$, and $4T_\eta$ for $\eta > 7.61$. In all cases we observe one impact per period T_η. Between these intervals the system undergoes period-doubling bifurcations leading to the multi-periodic behavior (up to period 50–$60T_\eta$) and chaotic motion. The black points in Fig. 6(a) denote the case of the soft impact modeling with the parameters $\alpha_s^2 = 100000.0$ and $h_s = 48.75$ (equivalent to the restitution coefficient $k_r = 0.6$ in hard impact modeling). Both diagrams are nearly identical. As it can be seen in Fig. 6(b) with the decrease of the base stiffness to $\alpha_s^2 = 2000$ and its damping to $h_s = 6.9$ the diagram (black points) does not change qualitatively. One observes small displacements of the thresholds of the low periodic behavior towards the lower values of the frequency η. Fig. 6(c) shows the same bifurcation diagram for smaller values of $\alpha_s^2 = 100.0$ and $h_s = 1.55$ (black points). Notice that the stiffness of the base is still 100 times larger than the stiffness of the beam. Further displacements of the thresholds of

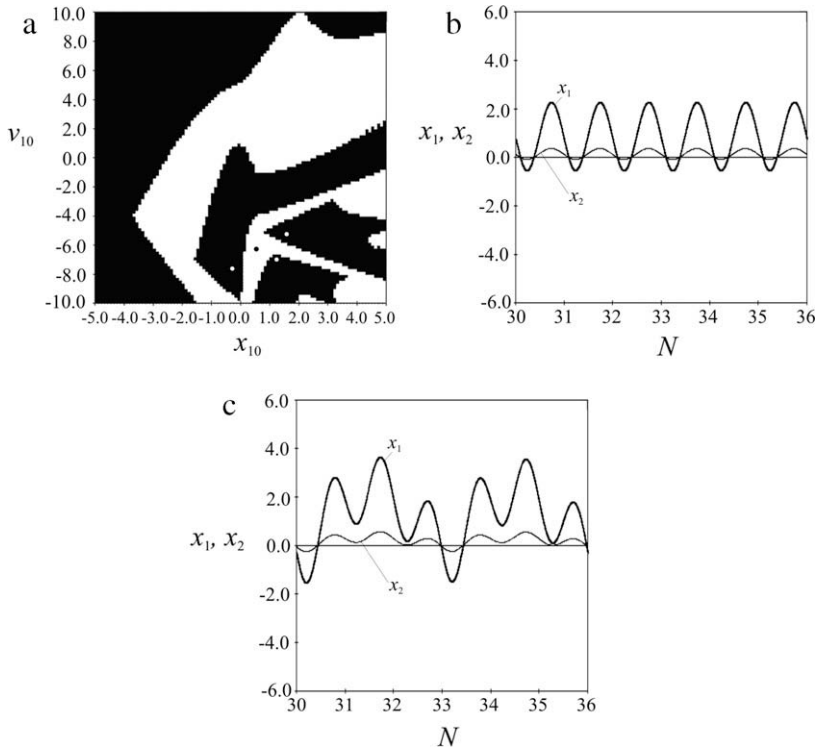

Fig. 7. Coexistence of two periodic attractors of 2DOF-1 system; $m_1 = 0.92$, $m_2 = 0.08$, soft impact model $\alpha_s^2 = 10$, $h_s = 0.488$, $\eta = 5.5$: (a) basins of attraction of T_η (white) and $3\,T_\eta$ periodic attractors, (b) time series of period T_η motion, (c) time series of period $3\,T_\eta$ motion.

the low periodic behavior are visible. We observe periodic motion with a period: T_η for $1.0 < \eta < 2.65$, $2T_\eta$ for $3.20 < \eta < 4.64$, $3T_\eta$ for $5.13 < \eta < 668$, and $4T_\eta$ for $\eta > 6.87$. The intervals with multi-periodic behavior become smaller. This type of behavior can be observed for $4.64 < \eta < 4.8$ and $6.68 < \eta < 6.87$. Further decrease of the base stiffness to $\alpha_s^2 = 10.0$ and $h_s = 0.488$ leads to the complete disappearance of these intervals as can be seen in Fig. 6(c). For $\eta = 2.61$ one observes period-doubling bifurcation in which the periodic motion with period T_η is replaced by the periodic motion with period $2T_\eta$. The reverse bifurcation takes place for $\eta = 5.01$ and one observes a periodic behavior with a period T_η. Additionally for $\eta > 5.01$ we observe the co-existence of two different periodic attractors. Beside the T_η-periodic attractor shown in Fig. 6(d) one can observe $3T_\eta$-periodic attractor. The basins of attraction of both attractors are shown in Fig. 7(a). The basins of T_η-and $3T_\eta$-periodic attractors are shown, respectively, in white and black. The examples of the time evolutions on these attractors are shown in Fig. 7(b) (period T_η) and Fig. 7(c) (period $3T_\eta$). The displacements of the colliding mass and a fender are shown respectively in black and grey. Time is rescaled as the number of the periods of the excitation force N.

Fig. 8(a–c) shows the bifurcation diagrams for 2DOF-2 system with $m_1 = 0.28$ and $m_2 = 0.72$. The results for the hard impact case with $k_r = 0.6$ and $d = 0.0$ are shown in grey (Fig. 8(a–c)). Equivalent diagrams for the soft impact models described by: $\alpha_s^2 = 100000.0$ and $h_s = 48.75$, $\alpha_s^2 = 2000.0$ and $h_s = 6.9$, $\alpha_s^2 = 100.0$ and $h_s = 1.55$ are shown, respectively, in Fig. 8(a), (b) and (c). Notice that similarly as in the case of Fig. 6(a–d) one observes the displacements of the thresholds of low periodic behavior towards lower values of the frequency η (Fig. 8(b)) and the disappearance of multi-periodic and chaotic behavior (Fig. 8(c)).

5. Conclusions

We compare two different methods of impact modeling, namely hard and soft impacts, and their influence on the dynamical behavior of the vibro-impact systems in which the rigid body collides with an elastic base. The conditions which allow the same rate of energy dissipation in dynamical systems with soft and hard impacts have been derived. They allow the construction of various soft impact models equivalent to the hard impact model with a given restitution coefficient.

Our results allow to draw the important conclusions:

1. For the large values of the stiffness coefficient of the base both models give the same results.

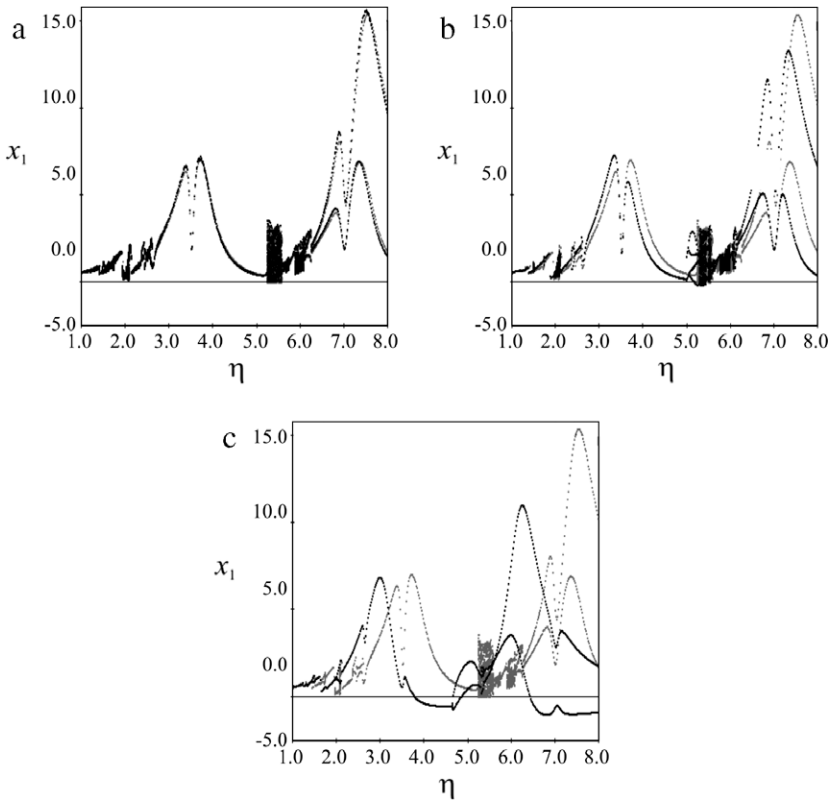

Fig. 8. Bifurcation diagrams showing the displacements of mass x_i observed at the time $t = nT_\eta = 2\pi/\eta$, ($n = 1,2,\ldots$) for 2DOF-2 system ($m_1 = 0.28$ and $m_2 = 0.72$), results for soft impact model with $k_r = 0.6$ are shown in grey, results for soft impact model are shown in black: (a) $\alpha_s^2 = 100,000$, $h_s = 48.75$, (b) $\alpha_s^2 = 2000$, $h_s = 6.9$, (c) $\alpha_s^2 = 100$, $h_s = 1.55$.

2. For lower values of this coefficient when the duration of body contact cannot be neglected the results of both methods diverge from each other. These differences occur as the result of external forces such as gravity, external excitation, which act on the colliding body during the contact. In hard impact modeling this effect is neglected.
3. In soft impact models one has to choose two independent parameters α_s^2 and h_s. Keeping the same rate of energy dissipation one can select the contact time and penetration depth as observed in the real experiment. This encourages the applications of new materials as elastic support for fenders [18–20].
4. The decrease of the base stiffness in the soft impact modeling leads to the simplification of the system behavior in the wide range of the external excitation frequency η. For the same rate of energy dissipation one observes only low periodic solutions. This observation allows chaos control in real engineering systems.

Acknowledgment

This study has been supported by the Polish Department for Scientific Research (DBN) under Project No. N501 037 31/2508.

References

[1] Kobrinskii AE. Dynamics of mechanisms with elastic connections and impact systems. London: Iliffle Book LTD; 1969.
[2] Feigin MI. Doubling of the oscillation period with c-continuous systems. Prikl Mat Mekh 1970;34:861–9.
[3] Filippov AF. Differential equations with discontinuous right-hand sides. Dordrecht: Kluwer Academic Publishers; 1988.
[4] Peterka F. Introduction to vibration of mechanical systems with internal impacts. Praha: Academia; 1981.
[5] Shaw SW, Holmes PJ. A periodically forced piecewise linear oscillator. J Sound Vibr 1983;90:129–55.
[6] Nordmark AB. Non-periodic motion caused by grazing incidence in an impact oscillator. J Sound Vibr 1991;145:279–97.
[7] Blazejczyk B, Kapitaniak T, Wojewoda J, Barron R. Experimental observation of intermittent chaos in a mechanical system with impacts. J Sound Vibr 1994;178:272–5.
[8] Lenci S, Rega G. A procedure for reducing the chaotic response region in an impact mechanical system. Nonlinear Dyn 1998;15:391–409.
[9] Hogan SJ. Heteroclinic bifurcations in damped rigid block motion. Proc R Soc Lond 1992;A439:155–62.
[10] Budd C, Dux F. Chattering and related behavior in impacting oscillators. Philos Trans R Soc 1994;347:365–89.
[11] Chin W, Ott E, Nusse HE, Grebogi C. Universal behavior of impact oscillators near grazing incidence. Phys Lett 1995;A201:279–97.
[12] Di Bernardo M, Feigin MI, Hogan SJ, Homer ME. Local analysis of C-bifurcation in *n*-dimensional piecewise-smooth dynamical systems. Chaos Solitons Fract 1999;10:1881–908.
[13] Ing J, Pavlovskaia E, Wiercigroch M. Dynamics of a nearly symmetrical piecewise linear oscillator close to grazing incidence: modeling and experimental verification. Nonlinear Dyn 2006;46:225–38.
[14] Ma Y, Agarwal M, Benerjee S. Border collision bifurcations in a soft impact system. Phys Lett A 2006;354:281–7.
[15] Ing J, Pavlovskaia EE, Wiercigroch M, Banerjee S. Experimental study of impact oscillator with one side elastic constraint. Philos Trans R Soc A 2008;366:679–704.
[16] Ma Y, Ing J, Banerjee S, Wiercigroch M, Pavlovskia E. The nature of the normal form map for soft impacting systems. Int J Non-linear Mech 2008;43:504–13.
[17] Czolczynski K, Blazejczyk-Okolewska B, Kapitaniak T. Dynamics of two degree-of-freedom cantilever beam with impacts. Chaos Solitons Fract 2009;40:1991–2006.
[18] Sitnikova E, Pavlovskaia EE, Wiercigroch M, Savi MA. Vibration reduction of the impact system by as SMA restraint: numerical studies. Int J Non-linear Mech, in press.
[19] dos Santos BC, Savi MA. Nonlinear dynamics of nonsmooth shape memory alloy oscillator. Chaos Solitons Fract 2007. doi:10.1016/j.chaos.2007.07.058.
[20] Sitnikova E, Pavlovskaia EE, Wiercigroch M. Dynamics of an impact oscillator with SMA constraint. Eur Phys J [Special Topics], accepted for publication.